Journal of Bioscience and Bioengineering
VOL. 128 No. 3, 337–343, 2019

ELSEVIER

www.elsevier.com/locate/jbiosc

Full-time dynamics of batch-wise enzymatic cycling system composed of two kinds of dehydrogenase mediated by NAD(P)H for mass production of chiral hydroxyl compounds

Tsuneo Yamane*

Graduate School of Biological and Agricultural Sciences, Nagoya University, Furo-cho, Chikusa Ward, Nagoya 464-8601, Japan

Received 28 January 2019; accepted 8 March 2019
Available online 5 April 2019

Enzymatic cycling system (coupled dehydrogenase-catalyzed biosystem being composed of two elementary enzymatic reactions mediated by NAD(P)H + NAD(P)$^+$) is industrially attractive for reducing prochiral carbonyl compounds to the corresponding chiral hydroxyl compounds. The reaction rate equation of the batch-wise biosystem was generally derived by ordered Bi Bi mechanism of two-substrate enzyme reaction on several reasonable assumptions. The rate equations of the batch-wise biosystem was generalized by transforming them into the dimensionless forms. The dimensionless forms were solved numerically. It was revealed that the batch-wise biosystem was generally made up of unique 3 phases, i.e., phases I, II and III. Phase I was very short transient so that the biosystem entered rapidly phase II. In phase II the consumption rate dynamically balanced with its formation rate so that the concentration of NAD(P)H was invariable with time (and hence NAD(P)$^+$ concentration was, too). Phase III was substrate-exhausting phase, and the coenzyme concentration became finally only [NAD(P)$^+$] or only [NAD(P)H] depending on the initial molar ratio of the prochiral carbonyl compound to the substrate of the coenzyme regeneration reaction ($[S]_0/[S']_0$) > or <1.0. In phases I and II the numerically calculated values of state variables were very close to the analytical but approximate ones. Preferable initial conditions of the batch-wise enzymatic cycling system, i.e., the initial coenzyme species = NAD(P)$^+$ and $[S]_0/[S']_0$<1.0, were proposed. As the main assumption irreversibility of the two elemental enzymatic reactions was discussed. Validity of the proposed rate equations was mentioned.

[**Key words:** Enzymatic cycling system; Coenzyme regeneration; Enzymatic coupled reaction; Oxidoreductase-catalyzed reaction; Dynamics of coupled two-enzyme reaction]

Enzymatic cycling system (oxidoreductase-catalyzed reactions involving enzyme-coupled coenzyme (such as NADH or NADPH) regeneration) (Fig. 1A) is composed of two elementary enzymatic reactions.

The product–synthesis reaction catalyzed by E is

$$S + X \xrightarrow{E} P + X' \qquad \text{(Reaction 1)}$$

And, the coenzyme (cofactor)-regeneration reaction catalyzed by E′ is

$$S' + X' \xrightarrow{E'} P' + X \qquad \text{(Reaction 2)}$$

The net reaction is obtained by summing up Reactions 1 and 2:

$$S + S' \rightarrow P + P' \qquad \text{(Reaction 3)}$$

Thus while its total concentration (= [X] + [X′]) is kept constant, the coenzyme circulates endlessly between Reactions 1 and 2 as far as both S and S′ exist. As E′, glucose-1-dehydrogenase (S′ is glucose) or formate dehydrogenase (S′ is formate) is mostly used. Sometimes E is called carbonyl reductase because Reaction 1 is reduction chemically.

The biosystem was first applied to determine trace amount of coenzyme in cell-free extracts in the area of analytical biochemistry (1). In nature, the coenzyme cycling is widely involved in living organisms. The most well-known coenzyme-cycling systems are observed in alcohol and lactic acid fermentations of glycolytic pathway. In the former case, alcohol dehydrogenase reduction (acetaldehyde + NADH + H^+ → ethyl alcohol + NAD^+) is coupled with glyceraldehyde-3-phosphate dehydrogenase oxidation (glyceraldehyde-3-phospate + NAD^+ → 1,3-bisphosphoglyceric acid + NADH + H^+), and in latter case lactate dehydrogenase reduction (pyruvate + NADH + H^+ → lactic acid + NAD^+) is coupled with glyceraldehyde-3-phosphate dehydrogenase oxidation.

Artificially designed coenzyme cycling system has recently been studied extensively because it is industrially attractive for reducing biochemically prochiral carbonyl compounds to the corresponding chiral hydroxyl compounds (2–5).

A number of advanced textbooks have been published so far concerning enzyme kinetics (6–10); however, all of them deal with only single enzyme system except the textbook by Cornish-Bowden (9). The reference has a chapter entitled “Multienzyme systems”. However, its content is a summary of metabolic engineering involving so called metabolic control analysis. Comprehensive

* Tel.: +81 52 789 4011; fax: +81 52 789 4012.
E-mail address: yamane.tsuneo@f.mbox.nagoya-u.ac.jp.

1389-1723/$ – see front matter
https://doi.org/10.1016/j.jbiosc.2019.03.004

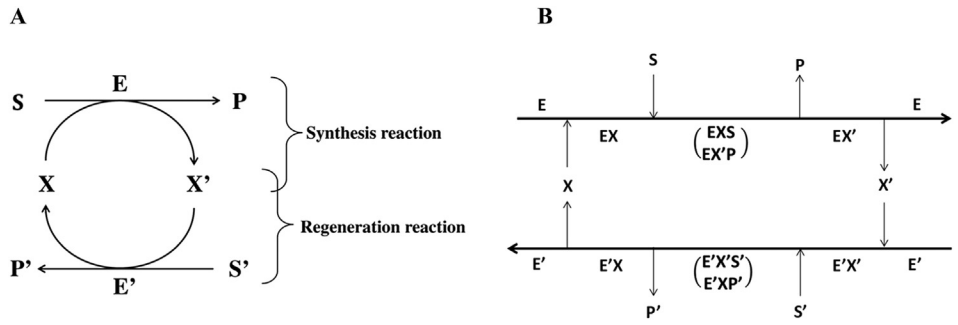

FIG. 1. (A) The general scheme of the enzymatic cycling system; (B) The graphical presentation of 'ordered Bi Bi mechanism' for the enzymatic cycling system according to the method proposed by Cleland (17). Rate constants are omitted.

kinetic analyses of various types of two-enzyme systems have been little described yet (even simple successive two-enzyme systems and parallel two-enzyme systems). Recently, Zhang et al. (11) presented a two-enzyme reaction (an FAD-dependent glucose oxidase and horseradish peroxidase) that generated complex dynamics. These were based on delayed self-adapting substrate competition, rather than on activation or inhibition.

The enzymatic cycling system is a unique two-enzyme reaction system coupled with each other mediated by NAD(P)H. No systematic engineering of the batch-wise enzymatic cycling system covering wide ranges of concentrations of both coenzymes (X and X′) and substrates (S and S′) has been studied yet. In order to reveal generally the engineering characteristics of the batch-wise enzymatic cycling system the aims of this study are, (i) to compare the numerical solutions with the analytical, but approximate solutions, (ii) to elucidate full-time dynamics of the coenzymes, substrates and products, and (iii) to propose a preferable operational condition of the batch-wise biosystem.

MATERIALS AND METHODS

Method of calculation Calculations of the analytical solution and of numerical solution of the simultaneous ordinary differential equation were carried out by a computational software program, Mathematica ver. 11.0, licensed for Nagoya University (Wolfram Research Inc., Champaign, IL, USA, 2016).

RESULTS AND DISCUSSION

General rate equation and dimensionless variables and parameters To derive the rate equation of the enzymatic cycling system, the following assumptions have been made: (i) E is highly enantiospecific for S, i.e., *e.e.* value of P is approximately 100%, (ii) both Reactions 1 and 2 are irreversible (i.e., the backward reaction rates of Reactions 1 and 2 are negligibly smaller than their forward reaction rates); (iii) the two dehydrogenase enzymes (E and E′) and the two forms of the coenzymes (NAD(P)H and NAD(P)$^+$) are stable during the batch operation; (iv) neither high-substrate-concentration inhibition nor product inhibition are observed; (v) the biosystem is carried out at a constant pH and at a constant temperature. The details of these assumptions will be argued later in the Discussion about the assumptions section.

Dehydrogenase-catalyzed irreversible reactions involving NAD(P)H (and NAD(P)$^+$) usually follow ordered Bi Bi mechanism (in which one form of the coenzyme is bound first to enzyme and another form of the coenzyme released last) (12–16). A graphical expression of the mechanism for the enzymatic cycling system is shown in Fig. 1B according to the method proposed by Cleland (17).

The rate equation of Reactions 1 and 2 with measurable kinetic constants is obtained on the quasi-steady state theory of binary and ternary complexes of enzyme and substrates such as EX and EXS. The quasi-steady state of the enzyme–substrate complexes reaches rapidly (usually in several seconds) and lasts until exhaustion of the substrate(s).

For the product–synthesis Reaction 1 with X=NAD(P)H, the rate is

$$\mathrm{Rate}_1 = \frac{k[\mathrm{E}]}{1 + K_x/[\mathrm{X}] + (1 + K_{ix}/[\mathrm{X}])\cdot K_s/[\mathrm{S}]} \tag{1}$$

And, for the coenzyme–regeneration Reaction 2 with X′=NAD(P)$^+$, the rate is

$$\mathrm{Rate}_2 = \frac{k'[\mathrm{E}']}{1 + K'_x/[\mathrm{X}'] + (1 + K'_{ix}/[\mathrm{X}'])\cdot K'_s/[\mathrm{S}']} \tag{2}$$

The rate of [X] is obtained from differential mass balance of [X] in completely stirred reaction mixture within a closed vessel:

$$\frac{\mathrm{d}[\mathrm{X}]}{\mathrm{dt}} = -\mathrm{Rate}_1 + \mathrm{Rate}_2 \tag{3}$$

In Eq. 3, the left side is accumulation rate of X, the first term of the right side is consumption (disappearance) rate of X and the second term is formation rate of X.

The conservation law of coenzymes, which is the most important constraint, is

$$[\mathrm{X}] + [\mathrm{X}'] = [\mathrm{C}] \tag{4}$$

where [C] is the total coenzyme concentration, i.e., [NAD(P)H] + [NAD(P)$^+$], which is invariable throughout a batch-wise enzymatic cycling system.

From the stoichiometry of the net Reaction 3,

$$[\mathrm{S}] + [\mathrm{P}] = [\mathrm{S}]_0 (= \text{const.}),\ [\mathrm{S}'] + [\mathrm{P}'] = [\mathrm{S}']_0 (= \text{const.}) \tag{5}$$

The initial condition of Eqs. 1–4 is:

$$[\mathrm{X}] = [\mathrm{X}]_0,\ [\mathrm{S}] = [\mathrm{S}]_0,\ [\mathrm{S}'] = [\mathrm{S}']_0,\ [\mathrm{P}] = [\mathrm{P}]_0 = 0,\ [\mathrm{P}'] = [\mathrm{P}']_0 = 0 \tag{6}$$

The variables and parameters in Eqs. 1–6 are made dimensionless by the following Eqs. 7–9:

$$\frac{[\mathrm{S}]}{K_s} \equiv S,\ \frac{[\mathrm{S}']}{K'_s} \equiv S',\ \frac{[\mathrm{P}]}{K_s} \equiv P,\ \frac{[\mathrm{P}']}{K'_s} \equiv P',\ \frac{[\mathrm{C}]}{K_x} \equiv C,\ \frac{[\mathrm{X}]}{K_x} \equiv X,\ \frac{[\mathrm{X}']}{K'_x} \equiv X' \tag{7}$$

TABLE 1. The characteristics of three phases of the batch-wise enzymatic cycling system[a].

Phase	Characteristics	Time length	Changes in r, [P] and [S]
I	Transient	Very much short	$r\searrow$ converging to $r_{singular}$ when $r_{singular} < r_0 \leq 1.0$, $r\nearrow$ converging to $r_{singular}$ when $0 \leq r_0 < r_{singular}$
II	The consumption rate dynamically balances with the formation rate.	Quite long	r = const. ($\cong r_{singular}$) regardless the value of r_0. [P] $\nearrow$ and [S] $\searrow$ linearly with elapsed time.
III	Substrate-exhausting	Short	$r\nearrow$ and = 1.0 finally and the final [P] = $[S]_0$ when $[S]_0 < [S']_0$, $r\searrow$ and = 0 finally and the final [P] < $[S]_0$ when $[S]_0 > [S']_0$.

[a] When $r_0 = r_{singular}$, phase I is not observed, when $[S]_0 \cong [S']_0$, clear phase III is not observed (r in phase III is slightly fluctuated around $r_{singlular}$, i.e., the biosystem is unstable), and when both $r_0 = r_{singular}$ and $[S]_0 \cong [S']_0$, phase I is not observed and r in phase III is slightly fluctuated around $r_{singlular}$. When $S_0 < 2$ (although the case is not attractive for mass production of P), clear phase II is not observed.

$$\frac{K'_x}{K_x} \equiv K\ ,\ \frac{K_s}{K_x} \equiv K_1\ ,\ \frac{K'_s}{K_x} \equiv K_2\ ,\ \frac{K_{ix}}{K_x} \equiv K_{i1}\ ,\ \frac{K'_{ix}}{K'_x} \equiv K_{i2} \tag{8}$$

$$\frac{k'[\mathrm{E}']}{k[\mathrm{E}]} = \frac{v'_{\max}}{v_{\max}} \equiv V,\ \ \frac{k[\mathrm{E}]}{K_x}\cdot t = \frac{v_{\max}}{K_x}\cdot t \equiv T \tag{9}$$

Furthermore, a novel dimensionless variable named redistribution factor, r, is introduced:

$$r \equiv \frac{[\mathrm{X}]}{[\mathrm{X}]+[X']}\left(\equiv \frac{[\mathrm{X}]}{[\mathrm{C}]} = \frac{X}{C} = \frac{X}{X+KX'}\right)\ \ (0 \leq r \leq 1) \tag{10}$$

From Eqs. 5, 7, 8 and 10, $X_0 = r_0 C$ and $X'_0 = (1-r_0)C/K$.

Approximate rate equation and summary of its analytical solution For comparison, the approximate rate equation and the results of its analytical solution (18) are summarized briefly.

When [S] and [S′] are assumed to be much greater than their Michaelis constants (K_s and K'_s), Eqs. 1 and 2 are reduced to

$$\mathrm{Rate}_{1a} \cong \frac{k[\mathrm{E}]}{1+K_x/[\mathrm{X}]}\ ,\ \ \mathrm{Rate}_{2a} \cong \frac{k'[\mathrm{E}']}{1+K'_x/[\mathrm{X}']} \tag{11}$$

The rate of [X] is

$$\frac{\mathrm{d}[\mathrm{X}]}{\mathrm{d}t} = -\mathrm{Rate}_{1a} + \mathrm{Rate}_{2a} \tag{12}$$

Using Eqs. 4–11, Eq. 12 is converted to:

$$\frac{\mathrm{d}r}{\mathrm{d}T} \cong -\frac{r}{1+rC} + \frac{V(1-r)}{K+(1-r)C}\ \ (0 \leq r \leq 1) \tag{13}$$

Equation 13 can be analytically solved as an implicit function, $T = \mathrm{f}(r)$. Equation 13 has also a singular solution, $r_{singular}$ which is unvarying with T:

$$r_{singular} = r_+ \text{ or } r_- \text{ or } r_1 \text{ depending on } V > 1 \text{ or } V < 1 \text{ or } V = 1 \tag{14}$$

In Eq. 14,

$$r_+ = \frac{1}{2}\left[1 - \frac{(K+V)}{C(V-1)} + \sqrt{\left\{1 - \frac{(K+V)}{C(V-1)}\right\}^2 + \frac{4V}{C(V-1)}}\right] \tag{15}$$

$$r_- = \frac{1}{2}\left[1 - \frac{(K+V)}{C(V-1)} - \sqrt{\left\{1 - \frac{(K+V)}{C(V-1)}\right\}^2 + \frac{4V}{C(V-1)}}\right] \tag{16}$$

$$r_1 = \frac{1}{K+1} \tag{17}$$

It has been concluded that the biosystem expressed by Eq. 13 can be divided into two phases, first phase I followed by phase II. In the phase II,

$$r_{\text{phase II}} \cong r_{singular}(\ = \text{const.}) \tag{18}$$

The dimensionless concentrations of the targeted product and the substrate, P_T and S_T at T, are

$$P_T \cong \left(\frac{K_x}{K_s}\right)\left(\frac{Cr_{singular}}{1+Cr_{singular}}\right)T,\ \ S_T \cong S_0 - \left(\frac{K_x}{K_s}\right)\left(\frac{Cr_{singular}}{1+Cr_{singular}}\right)T \tag{19}$$

Because $0 \leq S_T \leq S_0$, Eq. 19 is applicable only in the following range of T:

$$0 \leq T \leq S_0\left(\frac{K_s}{K_x}\right)\frac{\left(1+Cr_{singular}\right)}{Cr_{singular}} \tag{20}$$

Equation 20 predicts roughly the closing time of the batch-wise biosystem.

Numerical solution and its discussion The assumption that [S] and [S′] are much greater than their Michaelis constants (K_s and K'_s), i.e., [S] and [S′] are in the zero-th order reaction, is not satisfied in the real later stage of the batch-wise biosystem. The residual [S] and [S′] drop gradually to become very small. To get rid of the assumption one has to return to the original rate Eq. 3. By use of the dimensionless variables and parameters (Eqs. 7–9), Eq. 3 is transformed into the dimensionless form:

$$\frac{\mathrm{d}r}{\mathrm{d}T} = -\frac{N_1}{D_1} + \frac{N_2}{D_2} \tag{21}$$

Also the following dimensionless rate equations are obtained:

$$\frac{\mathrm{d}S}{\mathrm{d}T} = -\left(\frac{C}{K_1}\right)\frac{N_1}{D_1}\ ,\ \ \frac{\mathrm{d}S'}{\mathrm{d}T} = -\left(\frac{C}{K_2}\right)\frac{N_2}{D_2} \tag{22}$$

$$\frac{\mathrm{d}P}{\mathrm{d}T} = -\frac{\mathrm{d}S}{\mathrm{d}T}\ ,\ \ \frac{\mathrm{d}P'}{\mathrm{d}T} = -\frac{\mathrm{d}S'}{\mathrm{d}T} \tag{23}$$

In Eqs. 21 and 22,

$$N_1 = rS,\quad D_1 = (1+Cr)S + Cr + K_{i1} \tag{24}$$

$$N_2 = V(1-r)S',\quad D_2 = \{K + C(1-r)\}S' + C(1-r) + KK_{i2} \tag{25}$$

The set of Eqs. 21 and 22 is a first-order, homogeneous, nonlinear, simultaneous ordinary differential equation of 3 unknown variables (r, S and S') having 7 parameters (C, K, K_1, K_2, K_{i1}, K_{i2}, and V), and due to its nonlineality it cannot be solved analytically. Therefore, it was solved numerically by giving reasonable values of the parameters and the appropriate initial values of the variables. If K_2 is defined as $K_2 \equiv K'_s/K'_x$, $\mathrm{d}S'/\mathrm{d}T$ in Eq. 22 changes into $\mathrm{d}S'/\mathrm{d}T = -\{C/(K\cdot K_2)\}\cdot N_2/D_2$.

From a number of the numerical calculations with various sets of the values of the parameters and with various initial conditions, it has been revealed that the enzymatic cycling system is generally made up of unique and distinct 3 phases, i.e., phases I, II and III. The

division into these 3 phases has been especially noticeable in the time course of r. Change from the phase I to the phase II is clear and rapid, but transition from the phase II to the phase III is rather gradual. In the phase II the consumption rate of X ($rate_1$) dynamically balances with its formation rate ($rate_2$) so that $dr/dt = 0$, i.e., r = constant. It has been found that in phase III two cases of $[S]_0 < [S']_0$ and $[S]_0 > [S']_0$ (in dimensionless form, $K_1S_0 < K_2S'_0$ and $K_1S_0 > K_2S'_0$) give quite different profiles of r: when $[S]_0 < [S']_0$, r rises to unity finally, while when $[S]_0 > [S']_0$, r drops to zero finally. The characteristics of the three phases are summarized in Table 1.

For plotting typical curves of r, P and S vs. T by the numerical solution of Eqs. 21–23, values of the parameters, K, K_1, K_2, K_{i1}, and K_{i2}, were most plausibly decided by inference from the reported experimental data (12–15,19), especially from the data of L-leucine dehydrogenase (12) as E and of formate dehydrogenase as E′ (13). It was assumed that $C = 30$, which meant that [NAD(P)H] was 30 times higher than its Michaelis constant, K_x. It was also assumed that $V = 1.3$, which meant that v'_{max} of Reaction 2, $k'[E']$, was 1.3 times greater than v_{max} of Reaction 1, k [E].

Fig. 2 shows the typical numerical solutions of r vs. T of Eqs. 21 and 22 for the two cases, $[S]_0 < [S']_0$ and $[S]_0 > [S']_0$, together with the three phases, phases I, II, and III. Fig. 2 includes also the approximate solution (Eq. 13, dashed lines). Until the mid-time of the biosystem (phase I, followed by phase II), the approximate r almost equals the numerical r, i.e., they are indistinguishable. In Fig. 2A, r rises in the phase III to unity at the final stage. Contrarily, in Fig. 2B, r falls in the phase III to zero finally. Although the numerical solution exhibits these phenomena, the approximate solution gives only a horizontal line (dashed lines). These phenomena will be explained later in the next section.

As did the calculation of Eq. 13 (18), the numerical analysis of Eqs. 21 and 22 reveals also that from whichever value of r_0 the enzymatic cycling system may start, it converges to a constant value ($r_{singular}$) in a short time as shown in the insets of Fig. 2, and the biosystem enters the phase II. This means that as the initial coenzyme, X is not necessary but X′ or a mixture of X and X′ is equally effective, and the progress curves of r in the phase II and thereafter are the same irrespective of the values of r_0.

Fig. 3 shows typical progress curves of both S and P obtained by solving numerically Eqs. 21–23. Although the approximate analytical solution (Eq. 19 and Fig. 3, dashed lines) gives endless straight lines, the exact solution (Fig. 3, solid lines) shows plateau at the final time. The two lines are almost the same until the phase II, but the differences between them expand slightly and gradually in the phase III. The progress curves of both S and P can be approximately predicted by Eq. 19 until nearly the end. As shown in the insets of Fig. 3, in the phase I the lines of numerical solutions of both S and P are very slightly curved although the approximate S and P are straight lines from the beginning. There is no difference in progress curves between the two cases in the phase I as shown in the insets of Figs. 2 and 3. Eq. 19 and Fig. 3B indicate that the product concentration is approximately proportional to the reaction time until the end of the phase II.

To know whether the result of Table 1 is valid or not irrespective of the variations in [C], the numerical solutions have been performed at four levels of C, the results of which are shown in Fig. 4, indicating that three phases are observed at any value of C. The higher C is, the higher $r_{singular}$ is and the shorter the time length of the phase II is, since the $rate_1$ increases with increasing [C]. The time length of phase I is longer with increasing C and is the same between $r_0 = 0$ and 1 at each value of C (Fig. 4A, inset), although it is very short and r is almost vertical line on the full-time scale (Fig. 4A). Fig. 4B indicates that S and P are slightly different between the exact but numerical solution and approximate but analytical solution in phase II when C are small, but they are overlapped on the full-time scale when C is large. The phase III can be expressed only by the numerical solution as seen in Fig. 4.

To examine the effect of K on the biosystem, the numerical calculations were carried out for four levels of K (0.2, 0.5, 1.0, 5.0 and 10.0), the results of which are shown in Fig. 5. Fig. 5 indicates that the result of Table 1 is valid for these values of K. The value of $r_{singular}$ increases with decrease in K as suggested by Eq. 15 ($\partial r_+/\partial K$, $\partial r_-/\partial K$ and $\partial r_1/\partial K$ are negative irrespective of the values of C and V). However, when K is less than 1.0, the variations in r, P and S by the changes in K are rather little in this particular case. At smaller value of C, the changes in K affect more prominently the variations in r, P and S (calculated data no shown). Generally speaking, V is the more influential parameter than K (18). It is preferable that $V > 1.0$.

In carrying out an industrial batch-wise enzymatic cycling system for mass production of a chiral hydroxyl compound from its corresponding achiral carbonyl compound, the mathematical prediction described in this article proposes to start it up with $NAD(P)^+$ instead of NAD(P)H (not only because $NAD(P)^+$ is much cheaper than NAD(P)H, and but also because no matter how many r_0 may be, r converges to the same constant value) or with a mixture of NAD(P)H and $NAD(P)^+$ (if the mixture is cheaper than $NAD(P)^+$), and also with $[S]_0 < [S']_0$ (because only in this case S is completely converted to P) as well as with $V > 1.0$.

Discussion about the assumptions Equations 1 and 2 were derived from the assumptions 1–5. It is necessary to discuss them in detail for checking their validities. (i) Enantioselectivity of E toward S: If *e.e.* value of P is less than 100%, Reaction 1 is actually composed of two parallel reactions (S→(*S*)-form of P and S→(*R*)-form of P) so that the two synthetic reactions must be taken into consideration. Fortunately, literature survey shows that a number of E exhibit very good enantioselectivities. When *e.e.* value is less than 100% but very near 100%, the minor reaction can be ignored (assumption 1). (ii) Irreversibility of Reactions 1 and 2: If Reaction 1 is reversible, the rate equation is given by

$$\mathrm{Rate}_{1,\mathrm{reversible}} = \frac{V_1V_2([S][X] - [P][X']/K_{eq})}{\{K_{ix}K_sV_2 + K_xV_2[S] + K_sV_2[X] + (K'_xV_1/K_{eq})[P] + (K_pV_1/K_{eq})[X']}$$
$$+V_2[S][X] + (K_xV_2/K'_{ix})[S][X'] + (K'_xV_1/K_{ix}K_{eq})[P][X] + (V_1/K_{eq})[P][X']$$
$$+(V_2/K_{ip})[S][P][X] + (V_1/K_{is}K_{eq})[S][P][X']\} \quad (26)$$

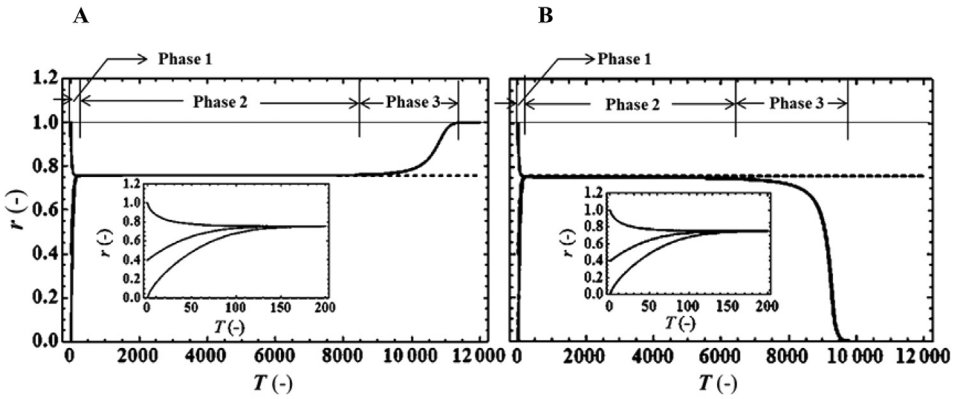

FIG. 2. Plots of r vs. T. (r_0 = 0, 0.4 and 1.0). (A) S_0 = 100, S'_0 = 130 (a case where $[S]_0 < [S']_0$); (B) S_0 = 100, S'_0 = 110 (a case where $[S]_0 > [S']_0$). The solid lines are the numerical solution of Eqs. 21 and 22, and the dashed lines are the analytical solutions of Eq. 13. The horizontal dashed lines are Eq. 15. The insets show the plots of r vs. T in the phase I (C = 30, K = 2.6, K_1 = 100, K_2 = 80, K_{i1} = 2.0, K_{i2} = 2.5, and V = 1.3).

where K_{eq} is the equilibrium constant, and V_1 and V_2 are the maximum rates of the forward and of backward reactions, respectively. Equation 26 contains the terms involving the product concentrations, [P] and [X′], and the total number of the parameters are 11 so that the rate Eq. 26 is very complex. Even when Reaction 1 is reversible, the numerical solution of the simultaneous differential equations is possible if the values of K_{eq} and of other 10 parameters are available. The literature survey tells us that in many cases the yields of P are nearly 100%, suggesting that the reaction is nearly irreversible. In many cases, water-immiscible organic solvents are used to increase hydrophobic S content in bioreactor (hence P content as well). The water/organic solvent biphasic system shifts the equilibrium reaction towards complete conversion. The substrate concentration [S] in the aqueous phase is low enough for the biosystem to be regarded as irreversible. Further study is required if Reaction 1 is truly reversible. As for Reaction 2, glucose-1-dehydrogenase is irreversible due to further spontaneous conversion of the product (D-glucono-1,5-lactone) to gluconic acid, and formate dehydrogenase is also irreversible because the product (CO_2) is eventually removed as CO_2 gas from the liquid reaction phase (assumption 2). (iii) Inhibitions by high-substrate-concentration and/or by the product: In industrial batch-wise biochemical production of chiral compounds, the substrate concentrations are quite high (0.2–2.0 M or more, or 50–300 g/L) to achieve as high final product concentrations as possible so that there might be possibilities of inhibitions by high-substrate-concentration and/or by the products. These inhibitions, if they occur, call for further modification of Eqs. 1 and 2. In some cases, the inhibitions can be eliminated or alleviated by liquid-liquid extraction, where majorities of substrates and/or products are in water-immiscible organic solvent. Also, the high-substrate-concentration inhibition can be avoided by its feeding or its intermittent addition to the reaction mixture (assumption 3). (iv) Instabilities of the enzymes and of the coenzymes: Literature survey tells us that the enzymatic cycling systems for mass productions of chiral hydroxyl compounds last as long as 6–240 h. During such long reaction times, E and/or E′ may lose more or less their activities, although no experimental data concerning that have not been reported so far. If their activities are lost according to the first-order decay model, the rate_1 and rate_2 should be modified as follows:

$$\text{Rate}_{1,\text{decay}} = \text{Rate}_1 \times \exp(-k_1 t),\ \text{Rate}_{2,\text{decay}} = \text{Rate}_2 \times \exp(-k_2 t) \quad (27)$$

where k_1 and k_2 are the first-order decay constants of E and E′, respectively. Numerical calculation of the simultaneous differential equations is possible if the values of k_1 and k_2 are available (assumption 4). (v) Constant pH and temperature: The optimal pH of E and of E′ are probably different. In that case, one has to set carefully pH value of reaction mixture possibly between them. When pH changes during the batch reaction, it must be controlled automatically at a constant value with acid or alkali by pH controller. That is especially important when E′ is glucose-1-dehydrogenase because its product is spontaneously hydrolyzed to gluconic acid, and when E′ is formate dehydrogenase because its substrate is sodium formate and Na^+ accumulates in the reaction mixture. The reaction temperature should be also carefully optimized by considering temperature dependency of each reaction rate (assumption 5).

Verifications of rate equations and Table 1 Eqs. 1 and 2 and the results of Table 1 can be verified by the following four items: (i) The whole development in this article are based on Eqs. 1 and 2. These equations are well worked out for the ordered Bi Bi mechanism (Fig. 1B) of NAD(P)H-dependent dehydrogenases (NAD(P)H binds first to the enzyme followed by the substrate S, and then the product P is released followed by $NAD(P)^+$ release last) (12–16). The general rate equation of reversible Reactions 1 and 2 is given by Eq. 26, and if the reactions are irreversible it is reduced to Eqs. 1 and 2. The irreversibility of Reactions 1 and 2 in the enzymatic cycling system has been already verified in the previous section. The differential equation of X given by Eq. 3 has been derived on the universal law of mass conservation. (ii) The phenomena that the products increased linearly with respect to reaction times were reported experimentally in a number of articles (19–23). The agreement between the reported data and the predictions shown in this study (Figs. 3, 4B and 5B) is one of supports that the kinetics proposed in this study is valid. (iii) The results shown in Fig. 2 are quantitatively consistent with the stoichiometry of the net Reaction 3. Reaction 3 infers that when $[S]_0 < [S']_0$, S is the limiting substrate and is completely converted to P finally, X being no longer converted to X′ so that all the coenzyme exists as X, while when $[S]_0 > [S']_0$, S′ is the limiting substrate and some amount of S remains unreacted at the end, resulting in the conversion of all X to X′ so that all the coenzyme exists as X′. The fact that the set of the differential equations (Eqs. 21 and 22) expresses well the stoichiometry of the net Reaction 3 is another support that the kinetics proposed in this study is valid. (iv) Enzymatic cycling system using two different kinds of enzyme has been exclusively studied in this study. There is so far no experimental data showing that $r \cong$ constant during long time (phase II) of batch-wise enzymatic cycling system using two enzymes. However, Itoh et al. (24) and Inoue et al. (25) reported

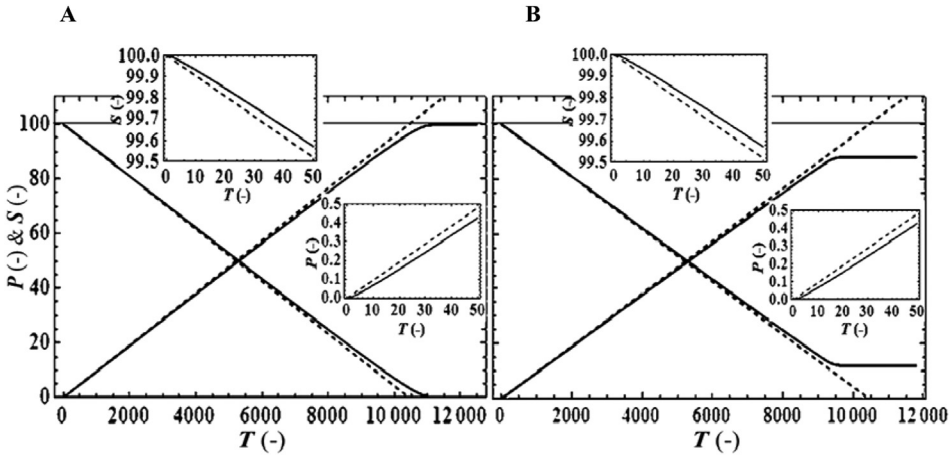

FIG. 3. Plots of both S and P vs. T when $r_0 = 0$. (A) $S_0 = 100$, $S'_0 = 130$ (a case where $[S]_0 < [S']_0$); (B) $S_0 = 100$, $S'_0 = 110$ (a case where $[S]_0 > [S']_0$). The solid lines are the numerical solution of Eqs. 21–23, and the dashed lines are calculated by Eq. 19. The lines with positive slopes are P and the lines with negative slopes are S. The insets show the plots of S and P vs. T in the phase I. The values of the parameters are the same as in Fig. 2.

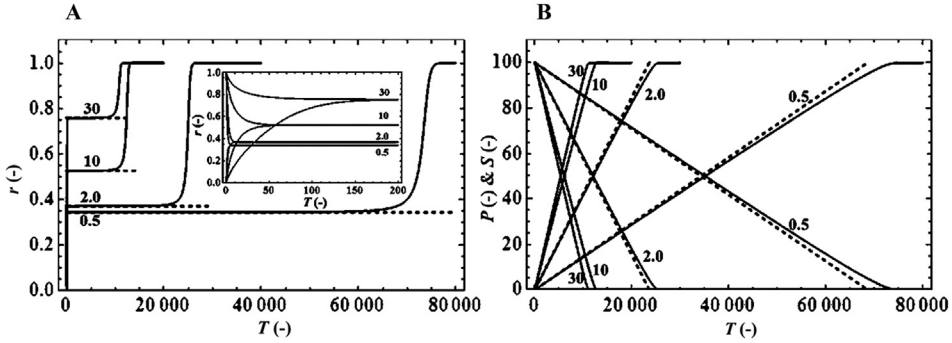

FIG. 4. Progress curves of r, P and S when $r_0 = 0$, and C =0.5, 2.0, 10 and 30. The solid lines are the exact, but numerical solutions and the dashed lines are the approximate, but analytical solutions. The numbers in the figures are the values of C. ($K = 2.6$, $K_1 = 100$, $K_2 = 80$, $K_{i1} = 2.0$, $K_{i2} = 2.5$, and $V = 1.3$), ($S_0 = 100$, $S'_0 = 130$). (A) Progress curves of r. The inset shows the plots of r vs. T in early reaction time showing the phase I ($r_0 = 1$ or 0); (B) progress curves of P (the lines with positive slopes) and of S (the lines with negative slopes). The lines of P and S for the numerical and analytical values when $C = 10$ and 30 overlap on the time scale of panel B.

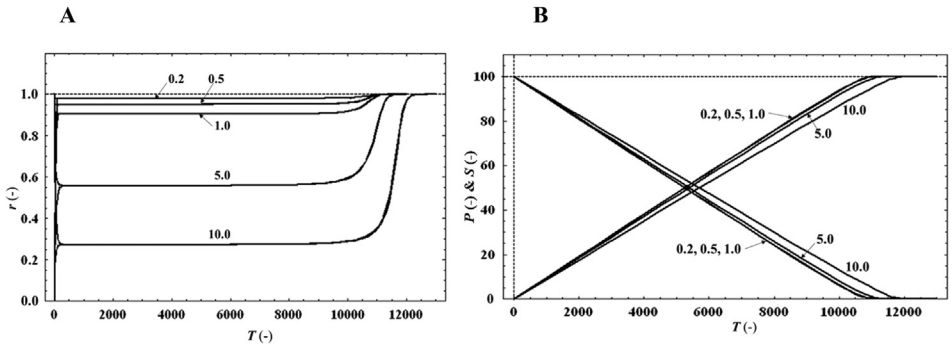

FIG. 5. Effect of K on the progress curves of r, P and S. The numbers in the figures are the values of K ($C = 30$, $K_1 = 100$, $K_2 = 80$, $K_{i1} = 2.0$, $K_{i2} = 2.5$, and $V = 1.3$) ($S_0 = 100$, $S'_0 = 130$). (A) Progress curves of r ($r_0 = 0$ or 1.0); (B) progress curves of P (the lines with positive slopes) and of S (the lines with negative slopes) ($r_0 = 0$). The lines for $K = 0.2$, 0.5 and 1.0 overlap each other.

that NAD^+ concentration became nearly constant during batch-wise chiral alcohol productions with a single dehydrogenase using 2-propanol as S′.

Although this study contains no experimental data and the numerical solution is based on the several assumptions, the results summarized in Table 1 and its discussions give us valuable information not only for planning logical experiments in laboratory but also for rational design and optimal operation of industrial mass production of chiral hydroxyl compounds. Further studies are required to verify the conclusion of Table 1 by determining experimentally the actual values of the parameters involved in Eqs. 1 and 2 and then by comparing the experimental data of the enzymatic cycling system in question with its mathematical simulation.

Nomenclature

[C]	total coenzyme concentration, i.e., [NAD(P)H] + [NAD(P)$^+$] defined by Eq. 4 (mM)
C	dimensionless total coenzyme concertation defined by Eq. 7 (−)
D_1, D_2	denominators defined by Eqs. 24 and 25
[E], [E′]	concentrations of E and E′ of Eqs. 1 and 2 (mM)
k, k'	k_{cat} of E and E′, of Eqs. 1 and 2
K, K_1, K_2, K_{i1}, K_{i2}	dimensionless values defined by Eq. 8 (−)
K_x, K'_x, K_s, K'_s, K_{ix}, K'_{ix}	kinetic constants of Eqs. 1 and 2 (mM)
N_1, N_2	numerators defined by Eqs. 24 and 25
r	redistribution factor defined by Eq. 10, $0 \leq r \leq 1$, (−)
[S], [P], [S′], [P′]	substrate and product concentrations (mM)
S, P, S', P'	dimensionless substrate and product concentrations defined by Eq. 7 (−)
t, T	time (s, or min, or h), dimensionless time defined by Eq. 9 (−)
[X], [X′]	concentrations of NAD(P)H and NAD(P)$^+$ (mM)
X, X'	dimensionless concentration of NAD(P)H and NAD(P)$^+$ defined by Eq. 7 (−)
V	$k'[E']/(k[E])$, dimensionless value defined by Eq. 9 (−)
Subscript 0	at time zero (i.e., $t = 0$)
Subscript T	at time T (−)

ACKNOWLEDGMENTS

The author declares no conflict of interest.

References

1. **Lowry, O. H., Passonneau, J. V., Schulz, D. W., and Rock, M. K.:** The measurement of pyridine nucleotides by enzymatic cycling, J. Biol. Chem., **236**, 2746−2755 (1961).
2. **Weckbecker, A., Gröger, H., and Hummel, W.:** Regeneration of nicotinamide coenzymes: principles and applications for the synthesis of chiral compounds, Adv. Biochem. Eng. Biotechnol., **120**, 195−242 (2010).
3. **Wang, Y., San, K.-Y., and Bennet, G. N.:** Cofactor engineering for advancing chemical biotechnology, Curr. Opin. Biotechnol., **24**, 994−999 (2013).
4. **Wu, H., Tian, C., Song, X., Liu, C., Yang, D., and Jiang, Z.:** Methods for the regeneration of nicotinamide coenzymes, Green Chem., **15**, 1773−1789 (2013).
5. **Kara, S., Schrittweiser, J. H., Hollmann, F., and Ansorge-Schumacher, M. B.:** Recent trends and novel concepts in cofactor-dependent biotransformations, Appl. Microbiol. Biotechnol., **98**, 1517−1529 (2014).
6. **Roberts, D. V.:** Enzyme kinetics. Cambridge University Press, Cambridge (1977).
7. **Nakamura, T.:** Enzyme kinetics. Society Publishing Center, Tokyo (1993) (in Japanese).
8. **Segel, I. H.:** Enzyme kinetics. John Wiley & Sons, New York (1993).
9. **Cornish-Bowden, A.:** Fundamentals of enzyme kinetics, 4th ed. John Wiley & Sons, New York (2013).
10. **Bisswanger, H.:** Enzyme kinetics: principles and methods, 3rd ed. John Wiley & Sons, New York (2017).
11. **Zhang, Y., Tsitkov, S., and Hess, H.:** Complex dynamics in a two-enzyme reaction network with substrate competition, Nat. Cat., **1**, 276−281 (2018).
12. **Ohshima, T., Misono, H., and Soda, K.:** Properties of crystalline leucine dehydrogenase from *Bacillus sphaericus*, J. Biol. Chem., **253**, 5719−5725 (1978).
13. **Kato, N., Sahm, H., and Wagner, F.:** Steady-state kinetics of formaldehyde dehydrogenase and formate dehydrogenase from methanol-utilizing yeast, *Candida boidinii*, Biochim. Biophys. Acta, **566**, 12−20 (1979).
14. **Mitamura, T., Urabe, I., and Okada, H.:** Enzymatic properties of isozymes and variants of glucose dehydrogenase from *Bacillus megaterium*, Eur. J. Biochem., **186**, 389−393 (1989).
15. **Peters, J., Minuth, T., and Kula, M.-R.:** Kinetic and mechanistic studies of a novel carbonyl reductase isolated from *Candida parapsilosis*, Biocatalysis, **8**, 31−46 (1993).
16. **Braumik, S. R. L. and Sonawat, H. M.:** Kinetic mechanism of glucose dehydrogenase from *Halobacterium salinarum*, Indian J. Biochem. Biophys., **36**, 143−149 (1999).
17. **Cleland, W. W.:** The kinetics of enzyme-catalyzed reactions with two or more substrates or products. I. Nomenclature and rate equations, Biochim. Biophys. Acta, **67**, 104−137 (1963).
18. **Yamane, T.:** Kinetics of batch-wise enzymatic cycling system for mass production of chiral compound, Biocatal. Biotransform., **35**, 315−328 (2017).
19. **Kataoka, M., Doi, Y., Sim, T.-S., Shimizu, S., and Yamada, H.:** A novel NADPH-dependent carbonyl reductase of *Candida macedoniensis*: purification and characterization, Arch. Biochem. Biophys., **294**, 469−474 (1992).
20. **Kizaki, N., Yasohara, Y., Hasegawa, J., Wada, M., and Shimizu, S.:** Synthesis of optically pure ethyl (*S*)-4-chloro-3-hydroxybutanoate by *Escherichia coli* transformant cells coexpressing the carbonyl reductase and glucose dehydrogenase genes, Appl. Microbiol. Biotechnol., **55**, 590−595 (2001).
21. **Yamamoto, H., Mitsuhashi, K., Kimoto, N., Kobayashi, Y., and Esaki, N.:** Robust NADH-regenerator; Improved α-haloketone-resistant formate dehydrogenase, Appl. Microbiol. Biotechnol., **67**, 33−39 (2005).
22. **Uzura, A., Nomoto, F., Sakoda, A., Nishimoto, Y., Kataoka, M., and Shimizu, S.:** Stereoselective synthesis of (*R*)-3-quinuclidinol through asymmetric reduction of 3-quinuclinone with 3-quinuclinone reductase of *Rhodotorula rubra*, Appl. Microbiol. Biotechnol., **83**, 617−627 (2009).
23. **Mitukura, K., Suzuki, M., Tada, K., Yoshida, T., and Nagasawa, T.:** Asymmetric synthesis of chiral cyclic amine from cyclic imine by bacterial whole-cell catalyst of enantioselective imine reductase, Org. Biomol. Chem., **8**, 4533−4535 (2010).
24. **Itoh, N., Matsuda, M., Mabuchi, M., Dairi, T., and Wang, J.:** Chiral alcohol production by NADH-dependent phenylacetaldehyde reductase coupled with *in situ* regeneration of NADH, Eur. J. Biochem., **267**, 2394−2402 (2002).
25. **Inoue, K., Makino, Y., and Itoh, N.:** Production of (*R*)-chiral alcohols by a hydrogen-transfer bioreduction with NADH-dependent *Leifsonia* alcohol dehydrogenase (LSADH), Tetrahedron Asymmetry, **16**, 2539−2549 (2005).